Apoptosis (2017) 22:1246–1259
DOI 10.1007/s10495-017-1394-y

Novel combination of salinomycin and resveratrol synergistically enhances the anti-proliferative and pro-apoptotic effects on human breast cancer cells

Jayant Dewangan[1] · Divya Tandon[1] · Sonal Srivastava[1] · Ajeet Kumar Verma[1] · Ashok Yapuri[1,2] · Srikanta Kumar Rath[1]

Published online: 26 July 2017

Abstract Resveratrol (RES) is a natural polyphenol having anti-proliferative activity against breast cancer cells. RES in combination with other chemo modulatory agents, minimizes toxicity and increases efficacy of the treatment. Salinomycin (SAL), a monocarboxylic polyether ionophore is known for selectively targeting breast cancer stem cells. Purpose of the present study was to investigate whether RES in combination with SAL exerts synergistic anti-proliferative activity on breast cancer cells. We further evaluated the molecular mechanism behind SAL and RES mediated cell death. Cytotoxicity assay was performed to determine 50% inhibitory concentration (IC50) of SAL and RES in different human breast cancer cells (HBCCs). Drug synergism and combination index (CI) were calculated using CompuSyn software and effects of synergistic combinations (CI < 1) involving lower doses of SAL and RES were selected for further studies. This combination significantly induced apoptosis in HBCCs without affecting non tumorigenic human breast epithelial cells MCF-10A. Co-treatment enhanced apoptosis in MCF-7 cells via reactive oxygen species (ROS) mediated mitochondrial dysfunction. Oxidative stress disrupt redox homeostasis which altered antioxidant enzymes viz. CuZn Superoxide dismutase (SOD), MnSOD and catalase. Additionally, combination altered nuclear morphology, enhanced PARP cleavage and led to caspase activation. SAL and RES also synergistically modulated MAPK pathway. Study suggests that SAL and RES offer a novel combination approach for the treatment of breast cancer.

Keywords Breast cancer · Salinomycin · Resveratrol · Apoptosis · Synergism · MAPK

Electronic supplementary material The online version of this article (doi:10.1007/s10495-017-1394-y) contains supplementary material, which is available to authorized users.

✉ Srikanta Kumar Rath
skrath@cdri.res.in

Jayant Dewangan
jayantdewangan@gmail.com

Divya Tandon
d.tandon84@gmail.com

Sonal Srivastava
sonal.srivastava24@gmail.com

Ajeet Kumar Verma
ajeetsonicdri@gmail.com

Ashok Yapuri
ashok.katravalli@gmail.com

[1] Genotoxicity Lab, Division of Toxicology, CSIR- Central Drug Research Institute, Sector -10, Jankipuram Extension, Lucknow, Uttar Pradesh 226031, India

[2] National Institute of Pharmaceutical Education and Research, ITI compound, Raebareli, Uttar Pradesh 229010, India

Introduction

Breast cancer is the leading cause of cancer death in women worldwide [1]. Current treatment for breast cancer includes chemotherapy, radiotherapy, surgery to excise tumor or breast tissue and hormone therapy [2]. Monoclonal antibodies, HER/EGFR inhibitors, PARP inhibitors, PI3K inhibitors, Insulin-like growth factor inhibitors and histone deacetylase inhibitors have been employed for breast cancer treatment [3, 4]. Despite of the availability of many chemotherapeutic drugs, development of resistance in various cancer types to these drugs poses a major challenge for the treatment of breast cancer [5]. A sub population of the cancer cells, known as cancer stem cells (CSCs), play a central

role in progression and reoccurrence of tumor due to development of drug resistance [6]. These cells become chemoresistant as they remain quiescent and escape cytotoxic therapy that targets rapidly dividing cells and are also capable of self-renewal and differentiation upon accumulation of mutation [7]. Therefore, employing drugs that target CSC population in tumor is crucial for effective treatment of cancer.

Salinomycin (SAL) is a polyether ionophore antibiotic showing anti-tumorigenic property in various types of cancer, including breast cancer [8], T-cell leukemia [9], colorectal cancer [10], prostate cancer [11] and hepatocellular carcinoma [12]. SAL sensitizes multidrug resistant cancer cells to chemotherapeutic agents [13]. Studies of Gupta et al. demonstrated the effect of SAL in selectively targeting breast cancer stem cells [14]. SAL was also shown to inhibit the CSC population in various cancer like lung, prostrate, colorectal and pancreas [15]. However, the use of high dose of SAL is restricted due to exhibition of some toxic effects. SAL was found to decrease fertility and induce dose-dependent toxicity in reproductive organs of male mice [16]. Neuronal cells damage and severe vacuolation in dorsal root ganglia of neurons was reported in horses exposed to SAL [17]. Therefore, identifying compounds having minimal toxic effects is necessary for the treatment of breast cancer and amelioration of side effects associated with chemotherapy.

Resveratrol (RES) is a natural polyphenol found in many dietary sources like grapes, pomegranate, berries, soy beans and peanuts [18]. This stilbene is synthesized by plants in response to injury or fungal attack [19]. RES was first isolated by Takaoka M.J. in 1940 from the medicinal plant *Veratrum grandiflorum O. Loes* [20]. Many fungal species like *Botryosphaeria, Penicillium, Cephalosporium, Aspergillus, Geotrichum, Mucor* and *Alternaria* also produce RES [21]. It exists in *cis* and *trans* isoform, in which *trans* is the major isoform and mainly found in red wine. The antioxidant and anti-inflammatory properties of RES have been shown to play a major role in the prevention of cardiovascular diseases [19]. Multiple studies have demonstrated the anti-cancer potential of RES in many types of cancers. RES selectively inhibits cyclo-oxygenase 2 expression [22], causes cell cycle arrest and induces apoptosis in breast cancer cells through various signalling mechanisms [23]. It is also known for chemo-sensitizing and enhancing the therapeutic efficacy of many drugs in various cancer treatment by different molecular pathways [24].

The rational of the present study was to study the effect of the combination of resveratrol and salinomycin in breast cancer cells. Individually, both the drugs exerted their anti-tumorigenic action by numerous molecular mechanisms like inhibition of Wnt/β-catenin, p53 dependent pathway, NF-kB, VEGF, and Stat-3 signaling or activation of ROS, MAPK and caspase dependent cell death [13, 18].

In the present study, we investigated the anti-proliferative combinatorial effect of SAL and RES in HBCCs (Human breast cancer cells). Experiments were extensively studied in MCF-7 cells. Our study revealed that the combination of SAL and RES act synergistically on HBCCs since, combination exerts enhanced apoptosis as compared to control and SAL or RES alone. Alteration in mitochondrial membrane potential (MMP), antioxidant enzyme expressions, nuclear morphology, caspase activation and ROS mediated activation of mitogen-activated protein kinases (MAPK) pathways were studied. The overall findings suggested that the combinatorial inhibitory effect of SAL and RES on HBCCs, was due to ROS mediated caspase activation, suppression of ERK, activation of JNK and p38 MAPKs signaling pathway.

Materials and methods

Chemicals

Salinomycin (S4526), resveratrol (R5010), RPMI-1640 medium (R4130), HEPES (H3375), gentamicin (G3632), sulforhodamine B (S1402), *N*-Acetyl-L-cysteine (A9165), trichloroacetic acid (T6399), cholera toxin (C8052), insulin (I5500), hydrocortisone (H4001) were purchased from Sigma-Aldrich. DMEM/F12 medium (12,400,024), Penicillin–Streptomycin solution (15,140,122), serum (16,000,044), EGF recombinant human protein (PHG0314), H2DCFDA (D-399) were obtained from Gibco Thermo Fisher Scientific.

Cell culture and maintenance

MCF-7, MDA-MB-231 and MCF-10A cells were obtained from Tissue and cell culture unit of CSIR-CDRI, Lucknow. MDA-MB-468 and T-47D were purchased from cell culture repository of National Centre for Cell Sciences, Pune. MCF-7, MDA-MB-231 and MDA-MB-468 were cultured in DMEM/F12 medium supplemented with 10% fetal bovine serum. T47D cells were cultured in RPMI medium along with 10% serum. MCF-10A cells were maintained in DMEM/F12 medium supplemented with EGF (20 ng/ml), Cholera toxin (100 ng/ml), Insulin (10 ng/ml), Hydrocortisone (0.5 µg/ml) and 5% horse serum. All the cells were cultured in humidified condition at 37 °C incubator in presence of 5% CO_2.

Cell viability assay

Cells were trypsinized and seeded into 96 well plate at density of 5000 cells per well. Next day cells were treated with SAL and RES, either alone or in combination. After 24 h of treatment, cytotoxicity assay were performed by sulforhodamine B (SRB) staining. Cells were fixed with 10% trichloroacetic acid for 1 h at 4 °C. Cells were washed with water

and dried, thereafter stained with SRB (Sigma-Aldrich) for 30 min. Cells were washed with 1% acetic acid, air dried and finally cell bound SRB was dissolved in 10mM tris base. Absorbance was taken at 510 nm on plate reader (BIOTEK). All the experiments were performed in triplicates.

Combination index analysis

Drug synergism studies were carried out using CompuSyn software version 1.0 (Ting Chao Chou and Nick Martin, Paramus, NJ, 2005). Combination index (CI) was measured based on mass action law of degree of drug interaction according to Chou and Talalay. It was calculated using formula CI=(D)1/(Dx)1+(D)2/(Dx)2, where (Dx)1 and (Dx)2 represents the dose of drug 1 and drug 2 in a combination which were required to achieve the same efficacy as that of drug 1 (D1) and drug 2 (D2) when used alone [25]. Human breast cancer cells (HBCCs) as well as normal human breast epithelial cells MCF-10A were treated with SAL and RES, either alone or in combination. Dose effect curve, Combination Index and DRI plots were generated through CompuSyn.

Evaluation of apoptotic morphology by light microscopy

Morphological observations of apoptosis or cell death were assessed after treating MCF-7 cells with SAL and RES, either alone or in combination for 24 h. Cells were observed under a Nikon phase-contrast light microscope and photographed.

Annexin V-FITC assay for apoptosis

MCF-7 and MCF-10A cells were seeded into 6 well plate at a density of 2×10^5 cells per well. Next day cells were treated with SAL and RES, either alone or in combination for 24 h. After treatment, cells were harvested by trypsinization and stained with Annexin V/FITC and propidium iodide (PI) in binding buffer according to manufacturer's protocol (BD Biosciences, Cat No. 556,547). Cells were analysed using flow cytometer (Becton Dickinson FACSCalibur). To assess ROS mediated apoptosis, cells were pre-incubated with 2mM *N*-Acetyl-L-cysteine (NAC) for 2 h before the SAL and RES treatment. Apoptosis evaluation was performed on NAC treated and untreated cells. These studies were carried out in three experimental repeats.

Chromatin condensation and nuclear morphology study

MCF-7 cells were seeded into 6 well plate and next day treated with SAL and RES, either alone or in combination for 24 h. Cells were washed with PBS (phosphate buffer saline) followed by 20 min fixation with 3.7% paraformaldehyde (pH 7.4). Cells were permeabilized with Triton X-100 for 15 min and stained with 1 µg/ml nuclear binding dye Hoechst 33,258 (H1398, Thermo Fisher Scientific). After three times washing with PBS images were acquired with fluorescence microscope (Nikon, Japan).

Estimation of ROS generation

Intracellular generated ROS in MCF-7 cells were analysed after SAL and RES treatment using fluorescent dye H2DCFDA. ROS converts this non-fluorescent moiety into fluorescent dichlorofluorescein (DCF). MCF-7 cells were seeded in 6 well plate and next day treated with SAL and RES, either alone or in combination. After 24 h of incubation, cells were washed with 1× PBS and stained with 10 µM H2DCFDA. Cells were incubated for 30 min at 37 °C in dark. The cells were washed with PBS and ROS was examined microscopically at 100× magnification (Nikon, Japan). For flow cytometry based ROS estimation, after treatment cells were harvested by trypsinization. Subsequently, incubated with H2DCFDA and analysed in flow cytometer. Each experiment were carried out in three independent repeats.

Detection of alteration in mitochondrial membrane potential

MMP was estimated using 2.5 µg/ml JC-1 fluorescent dye by flow cytometry. 0.2×10^6 MCF-7 cells were seeded in 6well plate. After 24 h, cells were treated with SAL and RES, either alone or in combination. Twenty-four hours post treatment, cells were harvested, washed with PBS and incubated with culture media containing JC-1 for 15 min at 37 °C in dark. Change in MMP was analysed using flow cytometer.

Caspase 3/7 activity

MCF-7 cells were seeded and grown in culture plates. Cells were treated with SAL and RES, either alone or in combination for next 24 h in CO_2 incubator. Cells were labelled with caspase 3/7 kit according to manufacturer's protocol (C10427, Thermo Fisher Scientific). In brief, cells were harvested by trypsinization, thereafter, CellEvent™ Caspase-3/7 green detection reagent was added to the cells and incubated for 30 min at 37 °C in dark. Caspase activity were analysed by flow cytometer. Caspase activity assay were done in three independent experimental repeats.

Immunoblotting

Whole cell lysates were prepared using CST cells lysis buffer. Protein concentration were quantified by Bradford

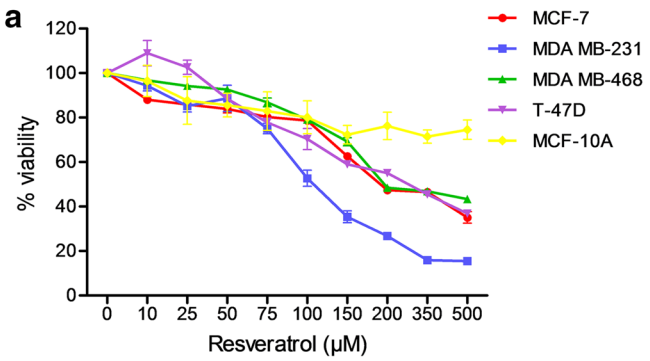

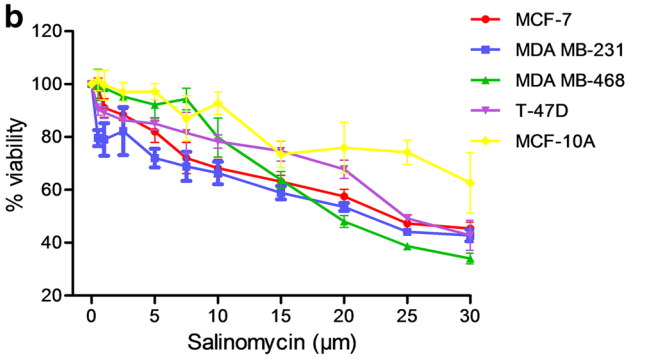

c

Breast cancer cells	IC50 (μM) ± S.D of SAL	IC50 (μM) ± S.D of RES
MCF-7	23.85 ± 0.80	146.9± 4.85
MDA MB-231	21.7 ± 0.47	105.3± 3.53
MDA MB-468	19.3 ± 0.87	133.5± 1.99
T-47D	24.75 ± 0.20	85.72± 11.12

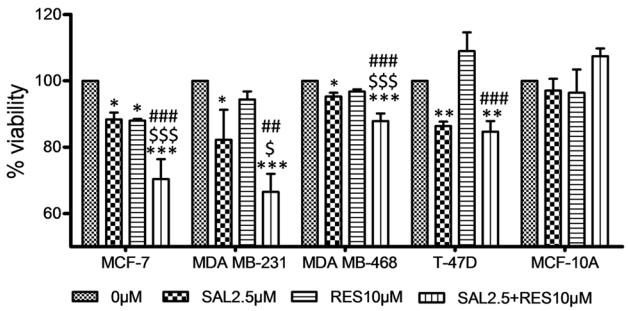

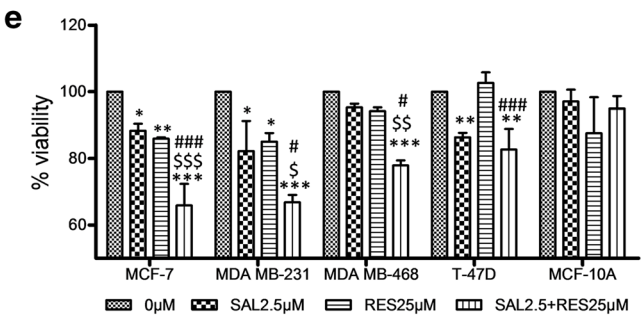

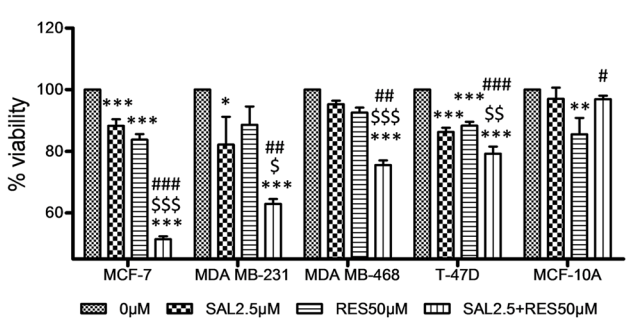

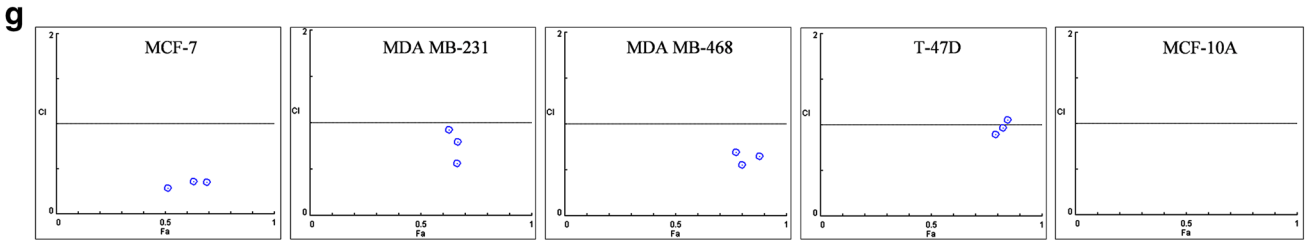

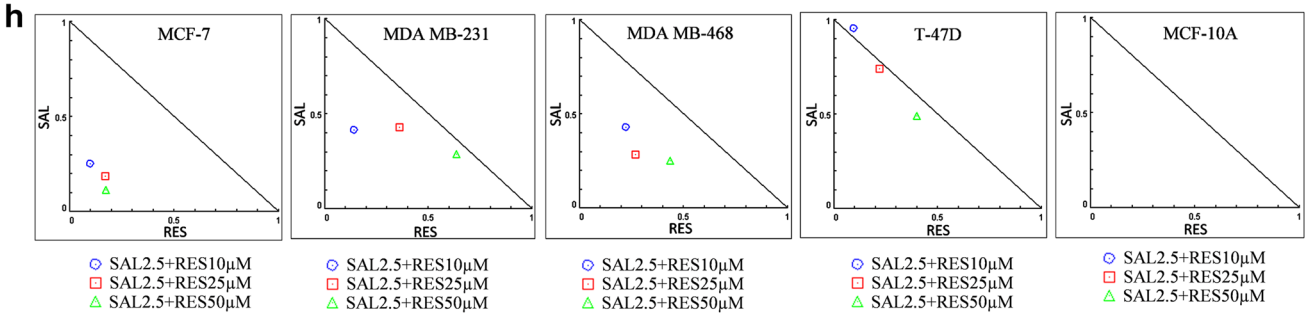

◂**Fig. 1** Salinomycin in combination with resveratrol inhibited growth of human breast cancer cells. (**a**, **b**) Effect of RES and SAL on cell viability of human breast cancer cells and **c** their IC_{50} value after 24 h of treatment. (**d**, **e**, **f**) Cell viability of different combinations of RES and SAL were assessed by SRB assay. Results were expressed as mean ± SD (n = 3). *P < 0.05, **P < 0.01, ***P < 0.001, calculated compared to control. $^{\$}$P < 0.05, $^{\$\$}$P < 0.01, $^{\$\$\$}$P < 0.001 with respect to individual SAL dose and $^{\#}$P < 0.05, $^{\#\#}$P < 0.01, $^{\#\#\#}$P < 0.001 with respect to individual RES dose. **g** The CI values for SAL and RES were calculated according to the Chou–Talalay's method by CompuSyn software at the 24 h time point, and plotted with the percent of cell growth inhibition as the fraction affected (Fa) cells. Each round symbol designated the CI value for each Fa at three different combination ratio in MCF-7, MDA-MB-231, MDA-MB-468, T-47D and MCF-10A cells. All the data are representative of three independent experiments. **h** Normalized isobologram for the combination of SAL and RES. Circle (*blue*), rectangle (*red*) and triangle (*green*) represents different combination ratio. Combination data point which fall *below the line* is synergistic, *above the line* is antagonistic or on the line is additive. (Color figure online)

reagent. 50 µg of protein sample were run on SDS–PAGE and transferred onto PVDF membrane. Membranes were blocked in 5% BSA for 1 h. After washing with 0.1% PBST, membranes were incubated with primary antibody overnight at 4 °C. Membranes were washed with PBST thrice and incubated with HRP conjugated secondary antibody for 2 h at room temperature. Antibodies used in experiment were phospho-ERK (sc-7976, santa cruz), ERK (sc-94, santa cruz), phospho-JNK (4671, cell signaling), JNK (9258, cell signaling), phospho-p38 (9211, cell signalling), p38 (9212, cell signalling), CuZnSOD (sc-11,407, santa cruz), MnSOD (S5569, Sigma-Aldrich), Peroxiredoxin 2 (PA3-751, Thermo Fisher scientific), HO1 (sc-10,789, santa cruz), catalase (C0979, Sigma-Aldrich), cleaved PARP (3140-100, biovision), cleaved caspase 7 (9491, cell signalling), cleaved caspase 8 (3258-100, biovision), cleaved caspase 9 (3149-100, biovision), Bcl-2 (3033-100, biovision) and actin (sc-1616-R, santa cruz). Blots were developed by enhanced chemi-luminescent detection reagent (G-Biosciences). Densitometry of blots were performed using Image J software. Experiments were carried out in triplicates.

Statistical analysis

All the data were analysed using GraphPad Prism version 5.00 for Windows, GraphPad Software, San Diego California USA. One-way ANOVA was used to measure statistical significance between control and treated groups and $p < 0.05$ were considered as statistically significant.

Results

Cytotoxic effect of SAL and RES on HBCCs

To investigate anti-proliferative activity of SAL and RES, human breast cancer cells were treated with different doses of respective drugs for 24 h. Results of cell viability showed that SAL and RES induce cytotoxic effect in human breast

Table 1 Combination Index values of SAL and RES combinations in human breast cancer cells

Drug combination	Combination index				
	MCF-7	MDA MB-231	MDA MB-468	T-47D	MCF-10A
SAL2.5 + RES10µM	0.35	0.55	0.62	1.05	2081.15
SAL2.5 + RES25µM	0.35	0.79	0.50	0.96	3.72
SAL2.5 + RES50µM	0.28	0.92	0.66	0.89	17.86

Combination index values were generated by CompuSyn software using formula CI = (D)1/(Dx)1 + (D)2/(Dx)2, where (Dx)1 or (Dx)2 represents the dose of drug 1 or 2 in a combination needed for achieving the same efficiency as that of the single drug 1 or 2 at D1 or D2, respectively. CI < 1 indicate drug synergism, CI > 1 antagonism and CI = 1 show additive effect

Table 2 Dose Reduction Index of SAL and RES of drug combinations in human breast cancer cells

Drug combination	Dose reduction index									
	MCF-7		MDA MB-231		MDA MB-468		T-47D		MCF-10A	
	SAL	RES	SAL	RES	SAL	RES	SAL	RES	SAL	RES
SAL2.5 + RES10µM	3.96	9.98	2.40	6.94	2.34	5.13	1.04	10.33	0.21	4.82E−4
SAL2.5 + RES25µM	5.30	5.82	2.32	2.74	3.85	4.06	1.34	4.40	2.49	0.30
SAL2.5 + RES50µM	8.86	5.66	3.48	1.56	4.23	2.30	2.03	2.45	1.81	0.05

Dose reduction index were generated from CompuSyn software. More than 1 DRI value show favourable drug combination

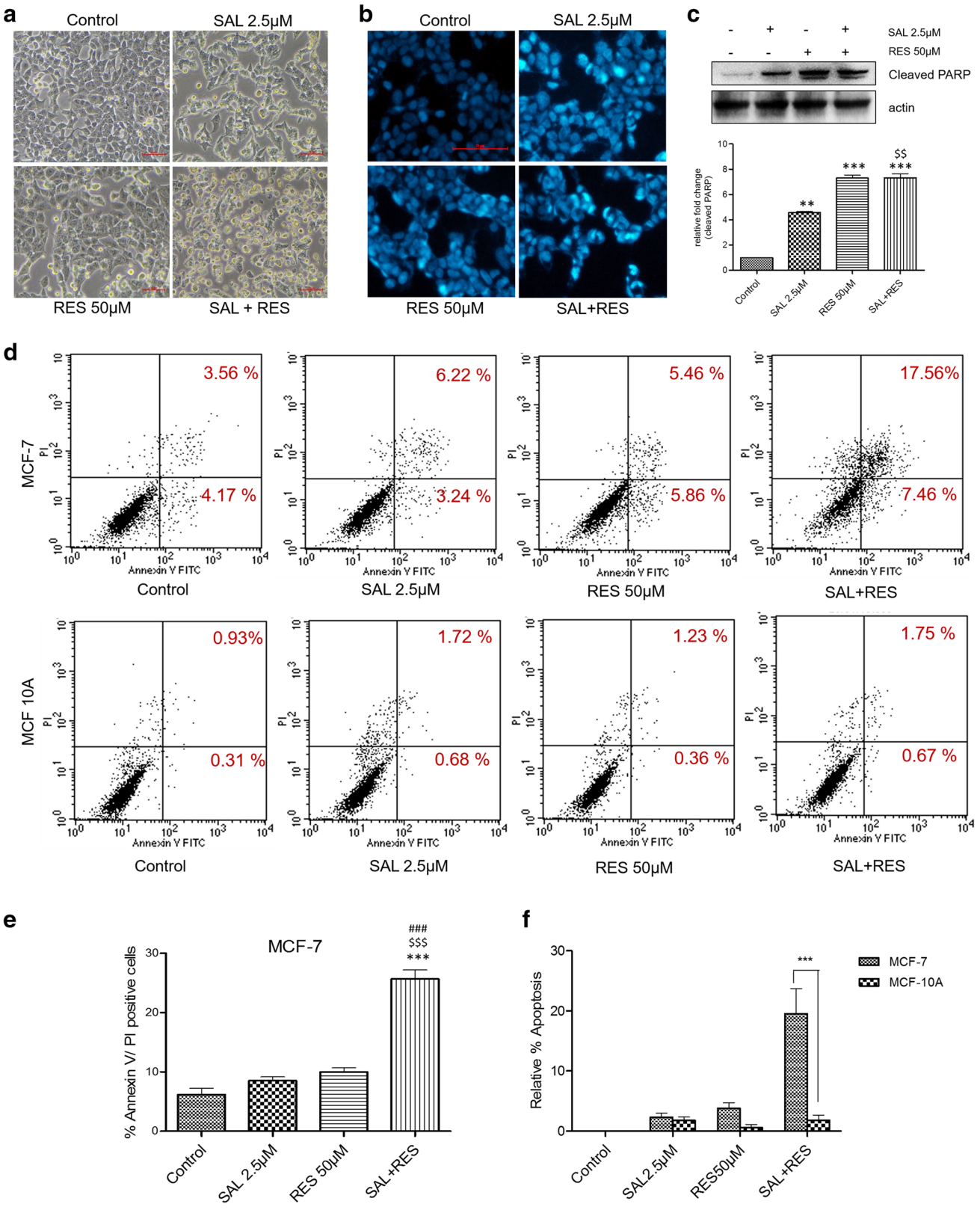
a
Control
SAL 2.5μM
RES 50μM
SAL + RES
b
Control
SAL 2.5μM
RES 50μM
SAL+RES
c
SAL 2.5μM
RES 50μM
Cleaved PARP
actin
relative fold change (cleaved PARP)
Control
SAL 2.5μM
RES 50μM
SAL+RES
d
MCF-7
MCF 10A
3.56 %
4.17 %
6.22 %
3.24 %
5.46 %
5.86 %
17.56%
7.46 %
0.93%
0.31 %
1.72 %
0.68 %
1.23 %
0.36 %
1.75 %
0.67 %
Annexin V FITC
PI
Control
SAL 2.5μM
RES 50μM
SAL+RES
e
MCF-7
% Annexin V/ PI positive cells
Control
SAL 2.5μM
RES 50μM
SAL+RES
f
Relative % Apoptosis
MCF-7
MCF-10A
Control
SAL2.5μM
RES50μM
SAL+RES

◂**Fig. 2** SAL and RES combination treatment efficiently and selectively induced apoptosis in human breast cancer cells. **a** Morphological examination of characteristic features of cell death of MCF-7 breast cancer cells. **b** Chromatin condensation and altered nuclear morphology were examined by Hoechst staining using fluorescence microscope in MCF-7 cells and **c** SAL and RES induced PARP cleavage in MCF-7 cells. **d** Apoptosis were analysed in human breast cancer cells MCF-7 and non-tumorigenic human breast epithelial cells MCF-10A after 24 h treatment with 2.5 μM SAL and 50 μM RES. **e** Statistical analysis of apoptosis in MCF-7 cells between untreated, single drug treatment and combination treatment. Results were expressed as mean ± SD (n = 3). *P < 0.05, **P < 0.01, ***P < 0.001, calculated compared to control. $^{\$}$P < 0.05, $^{\$\$}$P < 0.01, $^{\$\$\$}$P < 0.001 with respect to individual SAL dose and $^{\#}$P < 0.05, $^{\#\#}$P < 0.01, $^{\#\#\#}$P < 0.001 with respect to individual RES dose. **f** Statistical analysis of percentage of apoptosis induction between MCF-7 and MCF-10A cells. Significance were expressed as mean ± SD (n = 3). *P < 0.05, **P < 0.01, ***P < 0.001 between compared groups

cancer cells (Fig. 1a, b). Proliferation of MCF-7, MDA-MB-231, MDA-MB-468 and T-47D cells were reduced dose dependently with treatment of either drug. However, non-tumorigenic human breast epithelial cells MCF-10A were least affected by this combination treatment.

SAL and RES inhibited human breast cancer cell proliferation synergistically

Drug interaction relationship were studied using CompuSyn software. CI values in HBCCs were found less than 1 whereas the CI values in MCF-10A were more than 1. SAL and RES co-treatment in HBCCs viz. MCF-7, MDA-MB-231, and MDA-MB-468 and T-47D showed synergistic cytotoxic effect (Fig. 1d–f). SAL and RES co-treatment exhibited strong synergism in MCF-7 cells compared to other HBCCs as it generated lower CI value. Combination of 2.5 μM SAL and 50 μM RES inhibited cell proliferation effectively in MCF-7 cells and gave least CI value of 0.24. However, the CI values obtained inMCF-10A cells were more than 1. Drug synergism were represented with the help of combination index plot (Fig. 1f; Table 1) and isobologram (Fig. 1g). DRI values of each drug in combination treatment were obtained more than 1 (Table 2).

Morphological observation by light microscope

Cell morphology was observed under 100× magnification using bright field phase contrast microscope (Fig. 2a). Morphology of MCF-7 cells in SAL and RES combination treated group were observed unhealthy, as compared to untreated or alone drug treated group. Cell shrinkage and fragmentation of membrane bound apoptotic bodies were observed in combination treated MCF-7 cells, while untreated cells remain healthy. These changes were more notable as the drug treatment time increased.

Combination of SAL and RES induced apoptosis in breast cancer cells but not in non-tumorigenic breast epithelial cells

We determined the SAL and RES mediated apoptosis induction by Annexin V/PI staining using flow cytometric approach. As shown in Fig. 2d, 6.1% of untreated, 8.5% Sal treated and 9.9% res treated MCF-7 cells were stained positive for Annexin V/PI whereas a higher fraction of MCF-7 cells (25.6%) were positively stained when co-treated with SAL and RES combination for 24 h. However non- tumorigenic cells MCF-10A remained unaffected.

SAL and RES combination enhanced chromatin condensation

Chromatin condensation and apoptotic nuclear morphology were observed by fluorescent dye Hoechst-33258. Nucleus of untreated MCF-7 cells were stained dimly blue, nucleus were intact and round in shape, whereas combination treated MCF-7 nucleus were stained brightly and with altered morphology (Fig. 2b). These changes were found more in combination as compared to any of single drug used. These results demonstrated that the combination of SAL and RES effectively induced cellular apoptosis.

SAL and RES increased intracellular ROS generation

It is already reported that SAL increases intracellular ROS generation in breast cancer cells. To assess the involvement of ROS in SAL and RES mediated cytotoxicity in MCF-7 cells, it was stained with H_2DCFDA (2′,7′-dichlorofluorescin diacetate) and visualized under fluorescence microscope (Fig. 3a). Increased intracellular ROS level were found in combination treated cells as compared to untreated cells, which was further confirmed by flow cytometer (Fig. 3b). Pre-treatment of MCF-7 with NAC reduced percentage of Annexin V/PI positive cells in SAL and RES combination treated group (Fig. 3c) confirming ROS mediated apoptotic cell death.

SAL and RES depolarized MMP in MCF-7 cells

To elucidate whether SAL and RES induced apoptosis is mitochondria dependent, alteration in MMP was examined using JC-1 dye. Untreated cells were found with high JC-1 aggregates, which emit red colour. However, cells treated with SAL and RES combination expressed significant increase in JC-1 monomeric form, which emits green fluorescence. Data were represented in form of ratio of red: green fluorescence (Fig. 4).

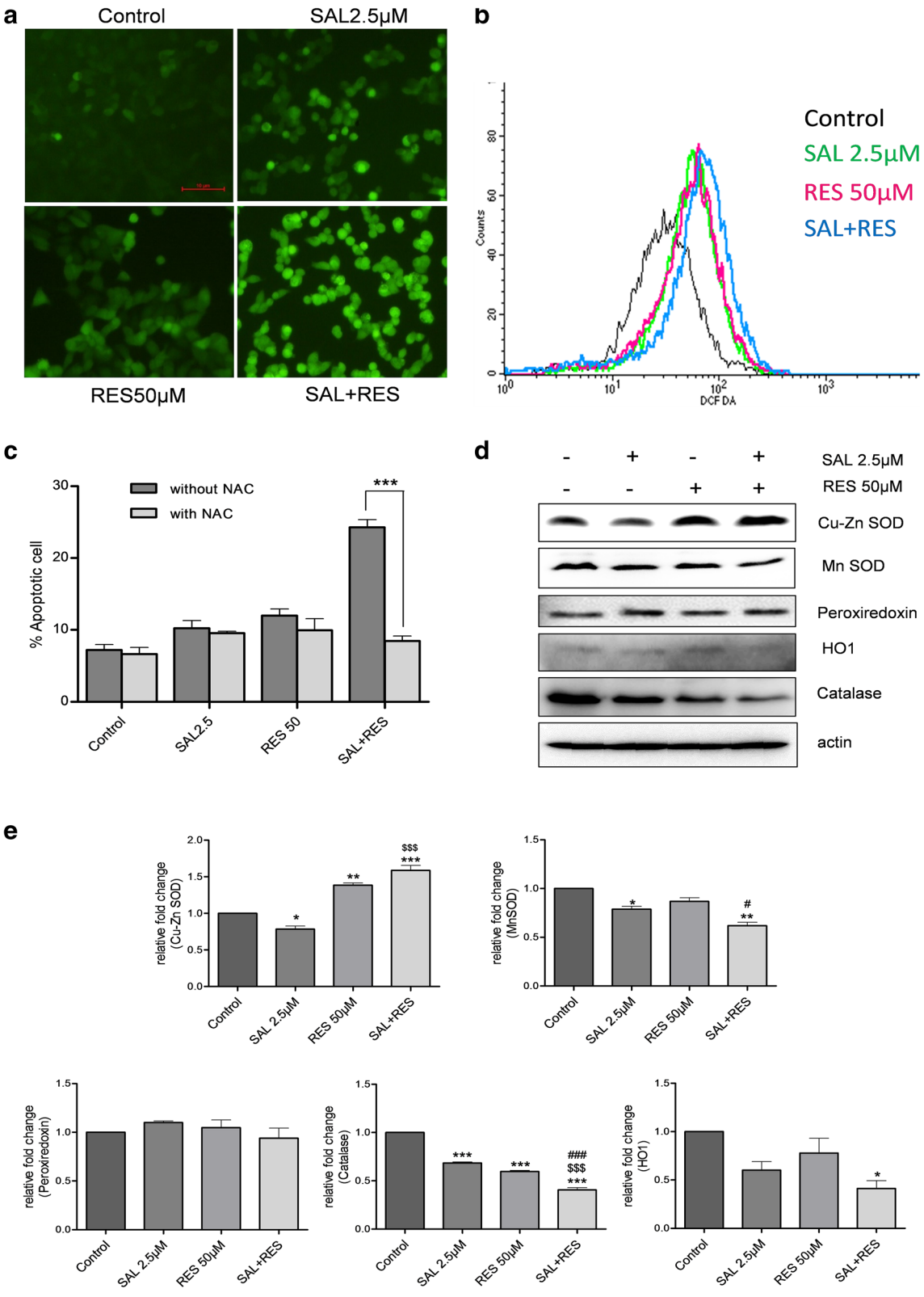
a
Control
SAL2.5μM
RES50μM
SAL+RES
b
Control
SAL 2.5μM
RES 50μM
SAL+RES
Counts
DCF DA
c
without NAC
with NAC
% Apoptotic cell
Control
SAL2.5
RES 50
SAL+RES
d
SAL 2.5μM
RES 50μM
Cu-Zn SOD
Mn SOD
Peroxiredoxin
HO1
Catalase
actin
e
relative fold change (Cu-Zn SOD)
relative fold change (MnSOD)
relative fold change (Peroxiredoxin)
relative fold change (Catalase)
relative fold change (HO1)
Control
SAL 2.5μM
RES 50μM
SAL+RES

◂**Fig. 3** SAL and RES induce ROS generation triggered apoptosis in human breast cancer cells. The intracellular ROS level were measured in MCF-7 cells using 10 μM H2DCFDA by **a** fluorescence microscopy and **b** flow cytometry. **c** Apoptosis level was decreased in MCF-7 cells by 2 h pre-treatment with ROS inhibitor *N*-acetyl-L-cysteine (NAC). Results were expressed as mean ± SD (n = 3) ***P < 0.001 between compared group. **d** , **e** Expression of antioxidant enzymes viz. CuZnSOD, MnSOD, peroxiredoxin 2, heme oxygenase 1 (HO1) and catalase were altered in MCF-7 cells by SAL and RES treatment. Results were expressed as mean ± SD (n = 3). *P < 0.05, **P < 0.01, ***P < 0.001, calculated compared to control. $^{\$}$P < 0.05, $^{\$\$}$P < 0.01, $^{\$\$\$}$P < 0.001 with respect to individual SAL dose and $^{\#}$P < 0.05, $^{\#\#}$P < 0.01, $^{\#\#\#}$P < 0.001 with respect to individual RES dose

SAL and RES combination triggered caspase mediated cell death

Caspase activation leads to induction of apoptosis in cells. Caspase 3/7 activity were evaluated after 24 h treatment of SAL and RES in MCF-7 cells. SAL or RES alone also potentiate caspase activation however, the combination of these two drugs promoted greater caspase 3/7 activation (Fig. 5a, b). Western blot analysis also confirmed that expression of caspase −7, −8 and −9 were significantly increased in combination group (Fig. 5c, d).

SAL and RES combination inhibited ERK phosphorylation and activated JNK-p38-MAPK pathway in breast cancer cells

ERK/JNK/p38 MAPK pathway plays critical role in maintaining cell growth and apoptosis. Therefore, we assessed the role of this pathway in SAL and RES induced apoptosis in MCF-7 cells. When MCF-7 cells were treated with 2.5 μm SAL and 50 μM RES together, ERK phosphorylation (Tyr 204) was effectively suppressed. On the other hand, phosphorylated-JNK (Thr183/Tyr185) and phosphorylated p38 (Thr180/Tyr182) levels were significantly elevated. However, effect of drug combination on MAPK was reversed after the treatment of NAC. These results suggest that SAL and RES induced apoptosis was influenced by MAPK pathway. (Fig. 6).

Discussion

Resveratrol plays a crucial role in sensitizing cancer cells to many chemotherapeutic agents [24]. Salinomycin is a monocarboxylic polyether ionophore antibiotic, commonly used in poultry industry as an anticoccidial drug. Its anticancer activity has been shown in multiple

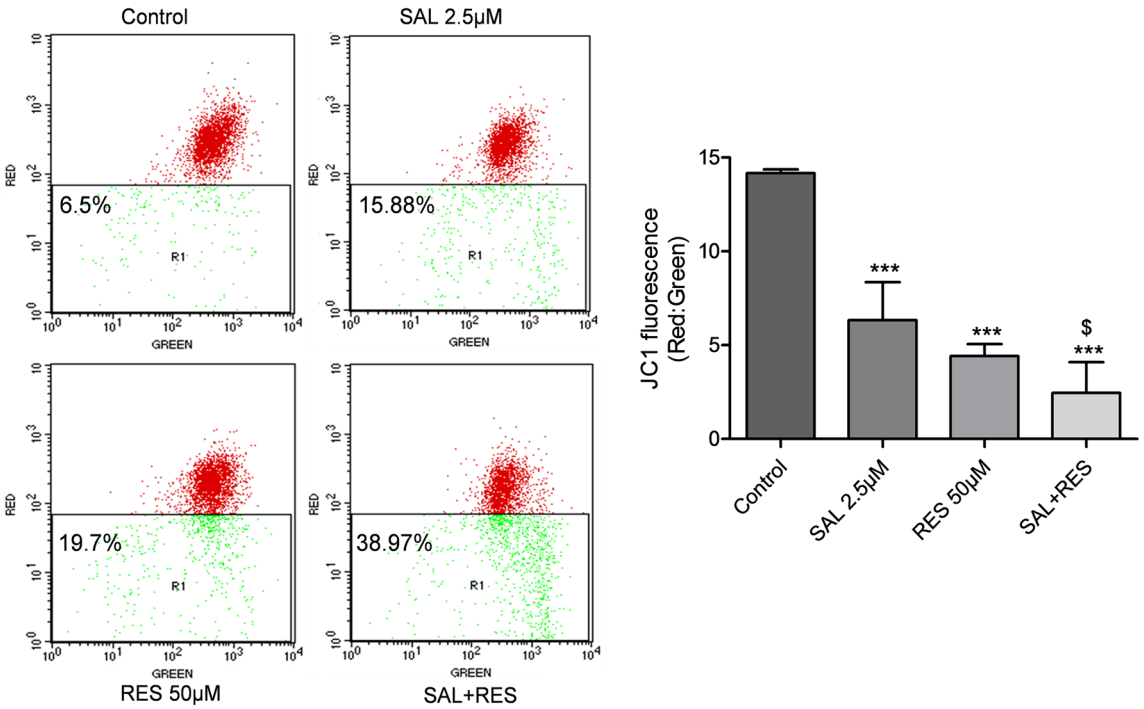

Fig. 4 Co-treatment altered mitochondrial membrane potential. SAL and RES co-treatment depolarized MMP of MCF-7 cells, which was detected by staining with JC-1 dye and analysed by flow cytometry. Data were represented in terms of ratio of *red* fluorescence: *green* fluorescence. Results were expressed as mean ± SD (n = 3). *P < 0.05, **P < 0.01, ***P < 0.001, calculated compared to control. $^{\$}$P < 0.05, $^{\$\$}$P < 0.01, $^{\$\$\$}$P < 0.001 with respect to individual SAL dose. (Color figure online)

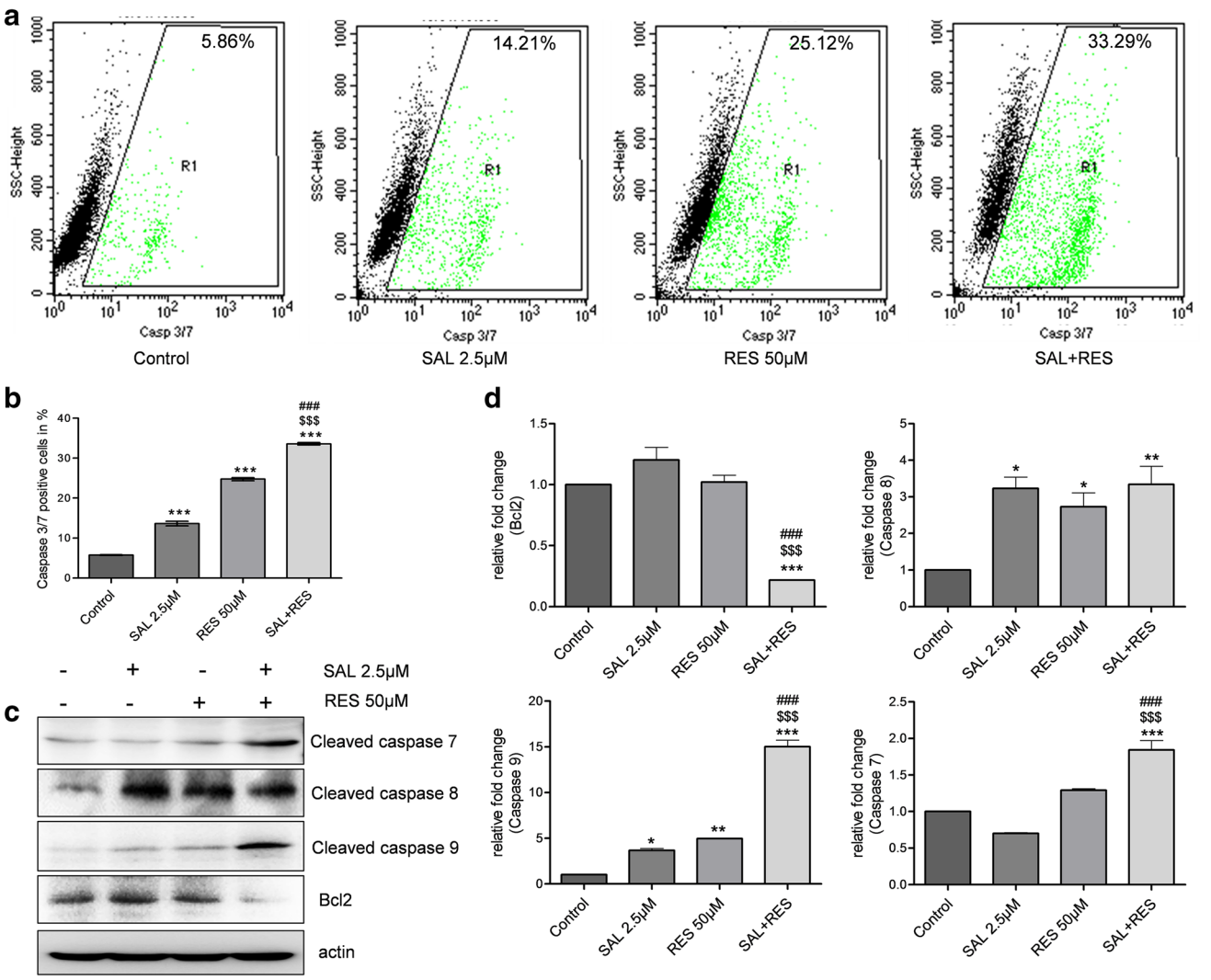

Fig. 5 SAL and RES induced apoptosis via caspase dependent apoptosis pathway. **a, b** Effect of 24 h co-treatment with SAL and RES in MCF-7 cells on caspase 3/7 activation. (**c**, **d**) Expression level of cleaved caspase-7, caspase-8, caspase-9 and anti-apoptotic protein Bcl2 were measured and normalized with actin in SAL and/or RES treated MCF-7 cells. Results were expressed as mean ± SD (n = 3). *P < 0.05, **P < 0.01, ***P < 0.001, calculated compared to control. $^{\$}$P < 0.05, $^{\$\$}$P < 0.01, $^{\$\$\$}$P < 0.001 with respect to individual SAL dose and $^{\#}$P < 0.05, $^{\#\#}$P < 0.01, $^{\#\#\#}$P < 0.001 with respect to individual RES dose

cancers. Interestingly, SAL selectively kills breast CSCs and chemo resistant tumor cells [14]. Combination of these drugs could be a more effective treatment of breast cancer. These studies demonstrate enhanced induction of apoptosis in human breast cancer cells upon co-treatment with SAL and RES.

In the present study, results have shown that resveratrol enhances anticancer potential of salinomycin in vitro. Experiments were carried out in different human breast cancer cells viz. estrogen receptor (ER) and progesterone receptor (PR) expressing MCF-7 and T-47D cells as well as ER and PR negative MDA-MB-231 and MDA-MB-468 cells [26]. Non-tumorigenic cell line MCF-10A were used to evaluate selective efficacy towards HBCCs of this combination. Cytotoxicity studies indicate that resveratrol and salinomycin have anti-proliferative effect in HBCCs irrespective of their receptor status (Fig. 1a, b). Combination of these drugs at lower dose illustrated greater growth inhibition and synergistic drug interaction (Fig. 1d–f). Drug synergism were studied using CompuSyn software (Ting Chao Chou and Nick Martin) and represented in terms of CI value and DRI plot (Tables 1, 2). Combination index value less than 1 (CI < 1) indicates synergistic drug interaction while more than 1 CI value (CI > 1) depicts drug antagonism. However combination index 1 (CI = 1) illustrates additive effect. Drug synergism is also represented in form of isobologram. It represents the equipotent combination of two drugs

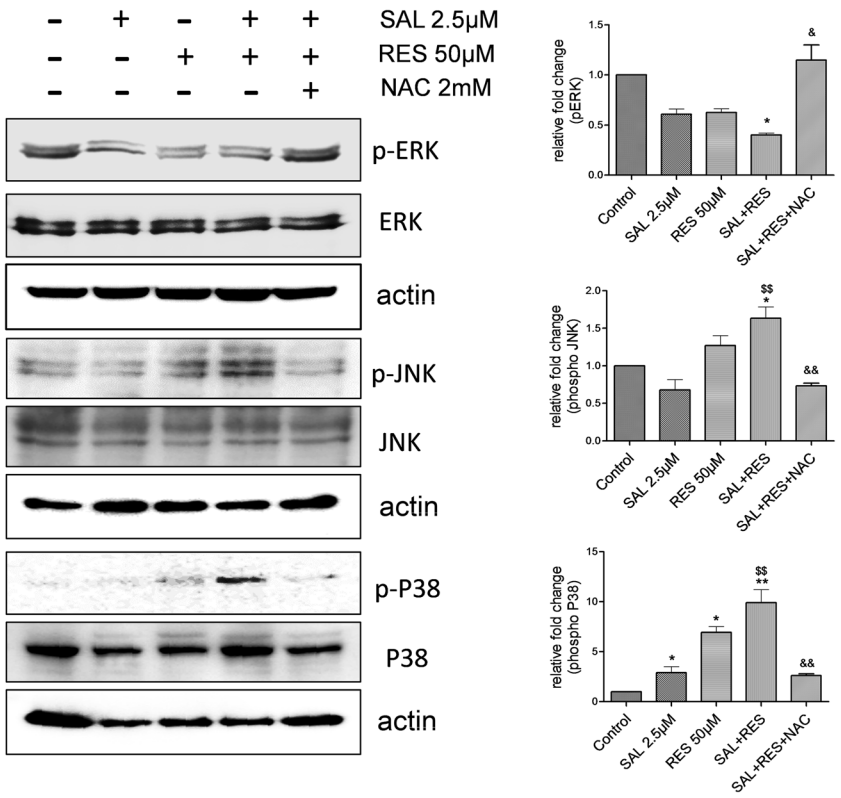

Fig. 6 MAPK signalling is involved in SAL and RES co-treatment induced cell death. Western blot analysis of MAPK signalling pathway was performed with proteins isolated from MCF-7 cells treated with SAL, RES, their combination and combination with NAC treatment for 24 h. ERK phosphorylation (p-ERK) were decreased whereas, phospho-JNK (p-JNK) and phospho-p38 (p-p38) expression were elevated in combination. p-ERK, p-JNK and p-p38 expression were normalized by dividing phospho protein to total expression. ERK and JNK were quantified by measuring expression of both the bands. Results were expressed as mean ± SD (n = 3). $^{*}P < 0.05$, $^{**}P < 0.01$, $^{***}P < 0.001$, calculated compared to control. $^{\$}P < 0.05$, $^{\$\$}P < 0.01$, $^{\$\$\$}P < 0.001$ with respect to individual SAL dose. $^{\#}P < 0.05$, $^{\#\#}P < 0.01$, $^{\#\#\#}P < 0.001$ with respect to individual RES dose. $^{\&}P < 0.05$, $^{\&\&}P < 0.01$, $^{\&\&\&}P < 0.001$ is significance between SAL + RES and SAL + RES + NAC

at different dose point. The dose points of drug combinations in breast cancer cells MCF-7, MDA-MB-231, MDA-MB-468 and T-47D inside the isobologram indicate drug synergism. One combination dose on T-47D cells showed slight additive effect (CI = 1.05) (Fig. 1g, h). However non-tumorigenic breast epithelial cell MCF-10A exhibited antagonistic drug interaction and showed normal growth pattern [27, 28]. DRI plot is the degree of measurement of how many fold single drug dose can be reduced when used in combination. All breast cancer cells showed more than 1 DRI value (DRI > 1) indicating favourable drug combination [29].

Structural alterations such as cell shrinkage, fragmentation into membrane bound apoptotic bodies and round shape floating cells are the morphological features of cell death [30]. MCF-7 cells were observed with above features in SAL and RES combination treatment group (Fig. 2a). These morphological observations suggest that treated cells were undergoing apoptosis. During early phase of apoptosis, membrane phospholipid phosphatidylserine switches from inner to outer leaflet of plasma membrane [31]. SAL and RES mediated apoptosis was confirmed by FITC tagged Annexin V and propidium iodide staining in MCF-7 cells. However, non-tumorigenic cells escaped from cell death (Fig. 2d, e). Furthermore, apoptosis results of MCF-7 versus MCF-10A depicted that the above combination selectively induced cell death in human breast cancer cells (Fig. 2f).

Mitochondria and peroxisomes are the key organelle which produce ROS as a result of normal cellular metabolism. Many antioxidant enzymes such as superoxide dismutase and catalase provide cellular protection against oxidative stress mediated cell damage [32]. However, expression of certain antioxidants alters during this condition. Disruption in redox homeostasis plays a major role in inducing apoptosis [33, 34]. Copper–zinc superoxide–dismutase (CuZnSOD) targets superoxide anion ($O_2^{\cdot -}$) in cytoplasm and peroxisome, while manganese superoxide–dismutase (MnSOD) encounters it in peroxisome and mitochondria. Superoxide dismutase converts $O_2^{\cdot -}$ into

hydrogen peroxide (H_2O_2). Further, H_2O_2 is neutralized into H_2O and O_2 by cytosolic and mitochondrial catalase [35]. Decrease in catalase expression leads to accumulation of ROS inside the cell, ultimately causing cell death [36]. Peroxiredoxin is also an important enzyme that plays a crucial role in protection against oxidative stress mediated cell damage by thioredoxin-dependent peroxidase activity [35]. Heme oxygenase-1 (HO1) is a cytoprotective enzyme which catalyses oxidative degradation of cellular heme. HO1 is highly expressed in various types of cancer [37]. Salinomycin induced ROS generation inhibited the growth of colon and breast cancer cells by ROS mediated apoptosis [38]. Combination of SAL and RES used in our study also potentiated induction of ROS in MCF-7 cells (Fig. 3a, b). SAL and RES combination increased CuZnSOD, which increased the level of superoxide inside the cell. Whereas decrease in the expression of MnSOD led to accumulation of H_2O_2, which was responsible for oxidative stress. HO1 was remarkably reduced but peroxiredoxin 2 was not significantly altered. Interestingly, catalase expression was also decreased, due to which H_2O_2 could not break down and the state of oxidative stress persisted inside the cells (Fig. 3d, e). However, SAL and RES induced apoptosis was significantly reduced by the pre-treatment with ROS scavenger NAC in MCF-7 cells (Fig. 3c). The findings suggest that resveratrol enhanced cytotoxic effect of salinomycin by involvement of ROS.

Cellular antioxidant system neutralizes ROS, however excessively produced ROS can cause disruption in MMP and cell death. Change in MMP activates caspase cascade. Caspases are the family of endoproteases that regulates inflammation and programmed cell death. There are two types of apoptotic caspases based on their mechanism of action: initiator caspases (like caspase-2, -8, -9 and -10) and executioner caspases (like caspase-3, -6 and -7) [39, 40]. Caspase 9 activated though intrinsic pathway, while caspase 8 activated through extrinsic pathway of apoptosis. Caspase 7 is a common effector caspase which performed cleavage of PARP and chromatin condensation in caspase 3 deficient MCF-7 cells [41, 42]. In our study we found that treatment of SAL and RES in MCF-7 cells, depolarized MMP (Fig. 4) and decreased expression of anti-apoptotic protein Bcl-2. This led to caspase-9, -8 and -7 activation (Fig. 5), chromatin condensation and PARP cleavage (Fig. 2c). Therefore, SAL and RES induced apoptosis is caspase dependent.

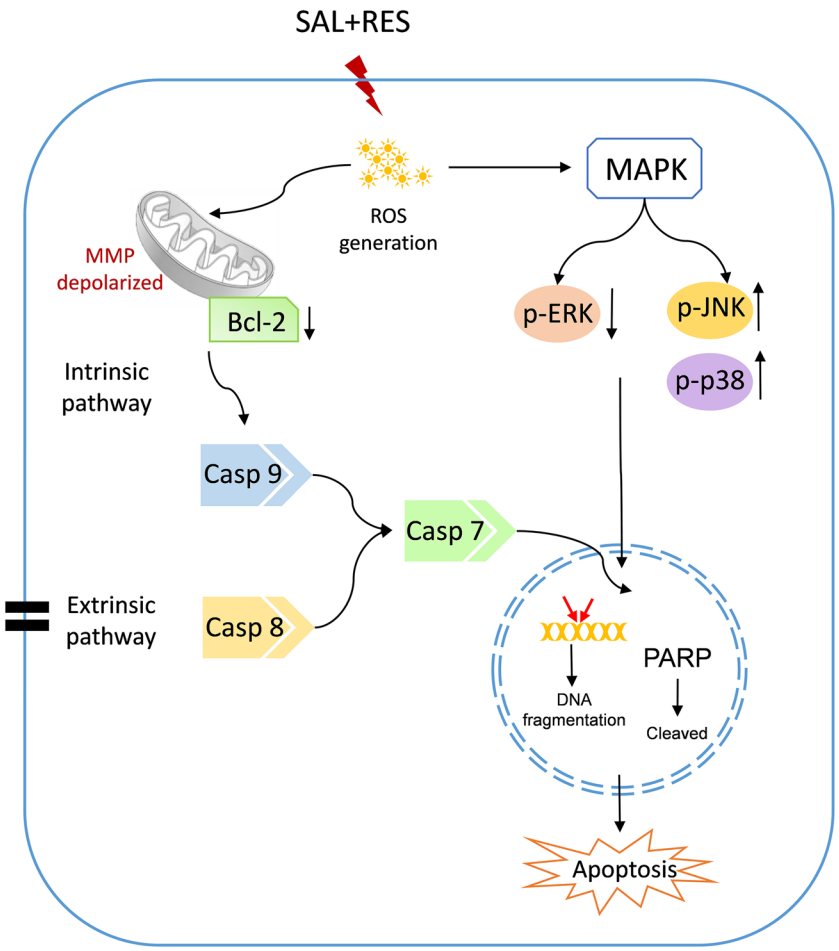

Fig. 7 Schematic representation of mechanism of anti-cancer action of SAL and RES co-treatment against HBCCs. SAL and RES synergistically enhance ROS generation in HBCCs which disrupts mitochondrial membrane potential thereby, increase caspase activation and PARP cleavage. Co-treatment also modulates MAPK pathway and induces apoptosis in HBCCs

ROS also activates MAPK pathway. The MAPK superfamily are protein kinases which consist of ERK, JNK and p38. MAPK responds to cellular stress and metabolism. ERK helps in cell survival whereas, p38 and JNK activation lead to apoptosis when subjected to oxidative stress [43]. This corresponds with the outcomes of our study (Fig. 6). In conclusion, overall findings suggested that SAL and RES combination induced apoptosis in HBCCs was influenced by ROS mediated caspase activation and involvement of MAPK pathway (Fig. 7). This novel combination could be a better therapeutic approach in breast cancer treatment. However, detailed further studies are required to elucidate effect of SAL and RES combination on human breast cancer.

Acknowledgements This work was supported by grants from Council of Scientific and Industrial Research, networking project BSC0103. J.D. gratefully acknowledge the fellowship received from University Grant Commission, New Delhi, A.K.V. and D.T. acknowledge the fellowship received from Council of Scientific and Industrial Research, S.S. acknowledge the fellowship received from Indian Council of Medical Research. Authors want to acknowledge Mr. A.L. Vishwakarma for support in flow cytometric studies. We are greatly thankful to Dr. Sharad Sharma for his valuable help in English editing of this manuscript. CSIR-CDRI communication number for this manuscript is 9514.

Author Contributions JD and SKR designed study, analysed data and prepared draft of manuscript. JD, DT, AY performed experimental work. SS and AKV helped in flow cytometer and data interpretation. All authors reviewed the manuscript.

Compliance with Ethical Standards

Conflict of interest The authors declare no competing financial interests.

References

1. Torre LA, Bray F, Siegel RL, Ferlay J, Lortet-Tieulent J, Jemal A (2015) Global cancer statistics, 2012. CA Cancer J Clin 65:87–108
2. Carter LG, D'Orazio JA, Pearson KJ. (2014) Resveratrol and cancer: focus on in vivo evidence. Endocr Related Cancer 21:R209–R225
3. Tinoco G, Warsch S, Gluck S, Avancha K, Montero AJ (2013) Treating breast cancer in the 21st century: emerging biological therapies. J Cancer 4:117–132
4. Higgins MJ, Baselga J (2011) Targeted therapies for breast cancer. J Clin Invest 121:3797–3803
5. Gottesman MM, Pastan I (1993) Biochemistry of multidrug resistance mediated by the multidrug transporter. Annu Rev Biochem 62:385–427
6. Suntharalingam K, Lin W, Johnstone TC et al (2014) A breast cancer stem cell-selective, mammospheres-potent osmium(VI) nitrido complex. J Am Chem Soc 136:14413–14416
7. Chen LS, Wang AX, Dong B, Pu KF, Yuan LH, Zhu YM (2012) A new prospect in cancer therapy: targeting cancer stem cells to eradicate cancer. Chinese. J Cancer 31:564–572
8. Jangamreddy JR, Ghavami S, Grabarek J et al (2013) Salinomycin induces activation of autophagy, mitophagy and affects mitochondrial polarity: differences between primary and cancer cells. Biochim Biophys Acta 1833:2057–2069
9. Fuchs D, Heinold A, Opelz G, Daniel V, Naujokat C (2009) Salinomycin induces apoptosis and overcomes apoptosis resistance in human cancer cells. Biochem Biophys Res Commun 390:743–749
10. Huczynski A, Janczak J, Antoszczak M, Wietrzyk J, Maj E, Brzezinski B (2012) Antiproliferative activity of salinomycin and its derivatives. Bioorg Med Chem Lett 22:7146–7150
11. Ketola K, Hilvo M, Hyotylainen T et al (2012) Salinomycin inhibits prostate cancer growth and migration via induction of oxidative stress. Br J Cancer 106:99–106
12. Wang F, He L, Dai WQ et al (2012) Salinomycin inhibits proliferation and induces apoptosis of human hepatocellular carcinoma cells in vitro and in vivo. PLoS ONE 7:e50638
13. Zhou S, Wang F, Wong ET et al (2013) Salinomycin: a novel anti-cancer agent with known anti-coccidial activities. Curr Med Chem 20:4095–4101
14. Gupta PB, Onder TT, Jiang G et al (2009) Identification of selective inhibitors of cancer stem cells by high-throughput screening. Cell 138:645–659
15. Dewangan J, Srivastava S, Rath SK (2017) Salinomycin: a new paradigm in cancer therapy. Tumour Biol 39:1010428317695035
16. Ojo OO, Bhadauria S, Rath SK (2013) Dose-dependent adverse effects of salinomycin on male reproductive organs and fertility in mice. PLoS ONE 8:e69086
17. Aleman M, Magdesian KG, Peterson TS, Galey FD (2007) Salinomycin toxicosis in horses. J Am Vet Med Assoc 230:1822–1826
18. Sinha D, Sarkar N, Biswas J, Bishayee A. (2016) Resveratrol for breast cancer prevention and therapy: preclinical evidence and molecular mechanisms. Seminars in cancer biology. Academic Press, Cambridge
19. Fremont L (2000) Biological effects of resveratrol. Life Sci 66:663–673
20. Baur JA, Sinclair DA. (2006) Therapeutic potential of resveratrol: the in vivo evidence. Nat Rev Drug Discov 5:493–506
21. Shi J, Zeng Q, Liu Y, Pan Z (2012) Alternaria sp. MG1, a resveratrol-producing fungus: isolation, identification, and optimal cultivation conditions for resveratrol production. Appl Microbiol Biotechnol 95:369–379
22. Subbaramaiah K, Chung WJ, Michaluart P et al (1998) Resveratrol inhibits cyclooxygenase-2 transcription and activity in phorbol ester-treated human mammary epithelial cells. J Biol Chem 273:21875–21882
23. Le Corre L, Chalabi N, Delort L, Bignon YJ, Bernard-Gallon DJ. (2005) Resveratrol and breast cancer chemoprevention: molecular mechanisms. Molecular Nutr Food Res 49:462–471
24. Gupta SC, Kannappan R, Reuter S, Kim JH, Aggarwal BB (2011) Chemosensitization of tumors by resveratrol. Ann N Y Acad Sci 1215:150–160
25. Chou TC (2006) Theoretical basis, experimental design, and computerized simulation of synergism and antagonism in drug combination studies. Pharmacol Rev 58:621–681
26. Holliday DL, Speirs V. (2011) Choosing the right cell line for breast cancer research. Breast Cancer Res 13:215
27. Chou TC, Talalay P (1981) Generalized equations for the analysis of inhibitions of Michaelis–Menten and higher-order kinetic systems with two or more mutually exclusive and nonexclusive inhibitors. European journal of biochemistry/FEBS 115:207–216
28. Chou TC, Talalay P (1984) Quantitative analysis of dose-effect relationships: the combined effects of multiple drugs or enzyme inhibitors. Adv Enzyme Regul 22:27–55

29. Chou TC (2010) Drug combination studies and their synergy quantification using the Chou–Talalay method. Cancer Res 70:440–446
30. Saraste A, Pulkki K (2000) Morphologic and biochemical hallmarks of apoptosis. Cardiovasc Res 45:528–537
31. Vermes I, Haanen C, Steffens-Nakken H, Reutelingsperger C (1995) A novel assay for apoptosis. Flow cytometric detection of phosphatidylserine expression on early apoptotic cells using fluorescein labelled Annexin V. J Immunol Methods 184:39–51
32. Michaeloudes C, Sukkar MB, Khorasani NM, Bhavsar PK, Chung KF (2011) TGF-beta regulates Nox4, MnSOD and catalase expression, and IL-6 release in airway smooth muscle cells. Am J Physiol Lung Cell Mol Physiol 300:L295–L304
33. Baluchamy S, Ravichandran P, Ramesh V et al (2012) Reactive oxygen species mediated tissue damage in high energy proton irradiated mouse brain. Mol Cell Biochem 360:189–195
34. Kim SJ, Jung HJ, Lim CJ (2011) Disruption of redox homeostasis and induction of apoptosis by suppression of glutathione synthetase expression in a mammalian cell line. Free Radic Res 45:1040–1051
35. Schrader M, Fahimi HD (2006) Peroxisomes and oxidative stress. Biochim Biophys Acta 1763:1755–1766
36. Patrushev N, Seidel-Rogol B, Salazar G (2012) Angiotensin II requires zinc and downregulation of the zinc transporters ZnT3 and ZnT10 to induce senescence of vascular smooth muscle cells. PLoS ONE 7:e33211
37. Chau LY (2015) Heme oxygenase-1: emerging target of cancer therapy. J Biomed Sci 22:22
38. Verdoodt B, Vogt M, Schmitz I, Liffers ST, Tannapfel A, Mirmohammadsadegh A (2012) Salinomycin induces autophagy in colon and breast cancer cells with concomitant generation of reactive oxygen species. PLoS ONE 7:e44132
39. Kumar S (2007) Caspase function in programmed cell death. Cell Death Differ 14:32–43
40. McIlwain DR, Berger T, Mak TW. (2013) Caspase functions in cell death and disease. Cold Spring Harbor Perspect Biol 5:a008656
41. Huang WR, Zhang Y, Tang X (2014) Shikonin inhibits the proliferation of human lens epithelial cells by inducing apoptosis through ROS and caspase-dependent pathway. Molecules 19:7785–7797
42. Germain M, Affar EB, D'Amours D, Dixit VM, Salvesen GS, Poirier GG (1999) Cleavage of automodified poly(ADP-ribose) polymerase during apoptosis. Evidence for involvement of caspase-7. J Biol Chem 274:28379–28384
43. Son Y, Cheong YK, Kim NH, Chung HT, Kang DG, Pae HO (2011) Mitogen-activated protein kinases and reactive oxygen species: how can ROS activate MAPK pathways? J Signal Transduct 2011:792639